Glycoprotein IIb/IIIa Receptor Imaging with ^{18}F-GP1 PET for Acute Venous Thromboembolism: An Open-Label, Nonrandomized, Phase 1 Study

Chanwoo Kim*[1], Jae Seung Lee*[2], Youngjin Han*[3], Sun Young Chae[1], Soyoung Jin[4], Changhwan Sung[1], Hye Joo Son[1], Seung Jun Oh[1], Sang Ju Lee[1], Jungsu S. Oh[1], Yong-Pil Cho[3], Tae-Won Kwon[3], Deok Hee Lee[5], Seongsoo Jang[6], Bohyun Kim[7], Norman Koglin[8], Mathias Berndt[8], Andrew W. Stephens[8], and Dae Hyuk Moon[1]

[1]Department of Nuclear Medicine, Asan Medical Center, University of Ulsan College of Medicine, Seoul, Republic of Korea; [2]Department of Pulmonology, Asan Medical Center, University of Ulsan College of Medicine, Seoul, Republic of Korea; [3]Department of Vascular Surgery, Asan Medical Center, University of Ulsan College of Medicine, Seoul, Republic of Korea; [4]Department of Nuclear Medicine, Nowon Eulji Medical Center, Eulji University, Seoul, Republic of Korea; [5]Department of Radiology, Asan Medical Center, University of Ulsan College of Medicine, Seoul, Republic of Korea; [6]Department of Laboratory Medicine, Asan Medical Center, University of Ulsan College of Medicine, Seoul, Republic of Korea; [7]Department of Laboratory Medicine, Soonchunhyang University Hospital Cheonan, Soonchunhyang University College of Medicine, Cheonan, Chungcheongnam-do, Republic of Korea; and [8]Piramal Imaging GmbH (now Life Molecular Imaging GmbH), Berlin, Germany

^{18}F-GP1 is a derivative of elarofiban with a high affinity to activated platelet glycoprotein IIb/IIIa and favorable in vivo characteristics for thrombus imaging in preclinical models. We aimed to explore the detection rate of thromboembolic foci with ^{18}F-GP1 PET/CT in patients with acute venous thromboembolism and to evaluate the safety, biodistribution, pharmacokinetics, and metabolism of ^{18}F-GP1. **Methods:** We studied patients who had signs or symptoms of acute deep-vein thrombosis (DVT) of the leg or acute pulmonary embolism (PE) within 14 d before ^{18}F-GP1 PET/CT and had thromboembolic foci confirmed by conventional imaging ($n = 10$ for DVT and $n = 10$ for PE). Dynamic whole-body PET/CT images were acquired for up to 140 min after injection of 250 MBq of ^{18}F-GP1. **Results:** ^{18}F-GP1 PET/CT was well tolerated, without any drug-related adverse events, and showed high initial uptake in the spleen, kidneys, and blood pool, followed by rapid clearance. The overall image quality was excellent and allowed interpretation in all patients. ^{18}F-GP1 PET/CT identified thromboembolic foci in all 20 patients with either DVT or PE. Vessel-level analysis revealed that ^{18}F-GP1 PET/CT detected 89% (68/76) of vessels with DVT and 60% (146/245) with PE. Importantly, ^{18}F-GP1 PET/CT showed increased uptake in 32 vessels that were not detected by conventional imaging, of which 25 were located in distal veins of the lower extremity in 12 patients. A positive correlation was found between ^{18}F-GP1 uptake and P-selectin–positive circulating platelets ($r = 0.656$, $P = 0.002$). **Conclusion:** ^{18}F-GP1 is a promising PET tracer for imaging acute venous thromboembolism in patients. ^{18}F-GP1 PET/CT may identify thrombi in distal veins of the leg, where conventional imaging has limitations.

Venous thromboembolism (VTE) is a disease that includes deep-vein thrombosis (DVT) of the leg or pelvis and its complication, pulmonary embolism (PE) (*1*). The highly variable and nonspecific symptoms and signs of VTE often result in delayed or inaccurate diagnosis (*2*), and most of the subset of fatal PEs die because of failure in diagnosis rather than inadequate therapy (*3*). For acute VTE, accurate and timely diagnosis is clearly critical to expedite the initiation of an effective therapeutic strategy (*4*). The performance of conventional imaging is excellent for detecting proximal DVT and PE but suboptimal for detecting thrombi in distal veins of the lower extremity (*5*), where the development of a thrombus occurs in most cases (*6*). In addition, it is currently difficult to precisely identify individuals who would benefit from prophylaxis, thus minimizing the risk of bleeding complications incurred by treatment of those at low risk (*1*); moreover, conventional diagnostic studies are not helpful in differentiating fresh thrombi from old organized ones (*7*). Incorrect diagnosis of recurrent VTE commits the patient to unnecessary prolonged anticoagulation therapy and results in higher risk and costs, whereas an incorrect conclusion that recurrent VTE is absent places the patient at high risk of potentially fatal PE (*4*).

A deposition of circulating platelets is a major component of the developing thrombus, and activated platelets have a high number of glycoprotein IIb/IIIa (GPIIb/IIIa) receptors. ^{18}F-GP1 is a novel ^{18}F-labeled derivative of the GPIIb/IIIa antagonist elarofiban, developed for imaging acute VTE with PET/CT. ^{18}F-GP1 binds specifically with a high affinity to activated GPIIb/IIIa (*8*). We aimed to explore the detection rate of thromboembolic foci with ^{18}F-GP1 PET/CT in patients with acute VTE and to evaluate its

safety, biodistribution, pharmacokinetics, and metabolism. We also assessed the correlation between quantitative uptake of ^{18}F-GP1 and clinical parameters, fibrinogen, and flow cytometric markers of platelet activation (P-selectin and activated GPIIb/IIIa).

MATERIALS AND METHODS

Study Design

This trial was a prospective, open-label, nonrandomized, single-center, single-dose exploratory study—and, to our knowledge, the first in humans—focused on assessing the safety, pharmacokinetics, biodistribution, and diagnostic performance of ^{18}F-GP1 PET/CT imaging in subjects with acute DVT or PE. Enrollment of 10 patients with DVT and 10 with PE was planned. Our study protocol was approved by the Ministry of Food and Drug Safety of Korea and by the Institutional Review Board of Asan Medical Center. This trial was registered at http://www.clinicaltrial.gov as NCT02864810 and was conducted in accordance with the Declaration of Helsinki and institutional guidelines. All subjects provided written informed consent before participating in the study.

Patients

We enrolled patients who had signs or symptoms of acute DVT of the leg or acute PE within 14 d before the ^{18}F-GP1 PET/CT study and with one or more thromboembolic foci confirmed by standard imaging modalities within 5 d before administration of ^{18}F-GP1 (Supplemental Table 1; supplemental materials are available at http://jnm.snmjournals.org).

Radiopharmaceutical Preparation

^{18}F-GP1 was synthesized by nucleophilic radiofluorination starting from the protected tosylate precursor using a non–cassette-type chemistry module (TRACERlab FXFN; GE Healthcare) as described recently (8).

^{18}F-GP1 PET/CT Image Acquisition

Oral hydration with water was encouraged before ^{18}F-GP1 PET/CT. Food restriction was not required. A radioactive dose of 250 ± 25 MBq of ^{18}F-GP1 at a total of no more than 10 μg was administered as a slow intravenous bolus for up to 60 s. Serial whole-body ^{18}F-GP1 PET/CT images covering vertex to toe were acquired using a Discovery 690 or 710 scanner (GE Healthcare). PET/CT data were reconstructed using the manufacturer-provided iterative algorithm. Additional details are provided in Supplemental Table 2.

Biodistribution and Image Analysis

^{18}F-GP1 PET/CT images were assessed visually and quantitatively by the consensus of 2 experienced nuclear medicine physicians who were informed of all standard imaging, clinical, and laboratory findings. For dynamic assessment of ^{18}F-GP1 biodistribution in normal organs, the volumes of interest of normal organs were drawn manually on dynamic fused PET/CT images. For thromboemboli, spheric volume of interests with a diameter of 12 mm were centered on the location of the maximum pixel value of ^{18}F-GP1. SUVs (g/mL) were defined as activity concentration (Bq/mL)/[injected activity (Bq)/body weight (g)].

Lesions with increased uptake in relation to background blood-pool activity were regarded as positive thromboembolic foci. Visual detection of DVT included analysis of common iliac, internal iliac, external iliac, common femoral, deep femoral, superficial femoral, popliteal, anterior tibial, posterior tibial, peroneal, and intramuscular calf (gastrocnemius and soleus) veins of the lower extremity (22 venous segments per patient). For PE, the main, lobar, and segmental pulmonary arteries were evaluated (25 arterial segments per patient). The capability of ^{18}F-GP1 PET/CT to detect acute VTE was assessed with standard imaging modalities serving as the gold standard. For lesion-based quantitative analysis, as many as 5 of the largest DVT lesions and 5 of the largest PE lesions on standard imaging were selected as reference lesions.

Safety Monitoring

For all participants, the safety of ^{18}F-GP1 was evaluated on the basis of laboratory parameters (Supplemental Table 3), vital signs, electrocardiograms, and physical examinations before and 3 h after intravenous administration of ^{18}F-GP1 and again at approximately 24 h. Adverse events were continuously recorded from the patient enrollment until adverse events were resolved, or up to a maximum of 28 d after the follow-up visit.

Fibrinogen Assay and Flow Cytometric Analysis of Platelet Activation

Details on the fibrinogen assay and flow cytometric analysis of platelet activation can be found in Supplemental Figure 1.

Statistical Analysis

Data are reported as mean ± SD unless specified otherwise. A P value of less than 0.05 was considered statistically significant. Detection rate and quantitative parameters were compared using the χ^2 and unpaired t test, respectively. Repeated-measures ANOVA was used to assess the time-dependent biodistribution of ^{18}F-GP1. The correlation of ^{18}F-GP1 uptake with quantitative parameters was assessed using the Pearson correlation coefficient. All statistical tests were conducted using SPSS Statistics (version 21, IBM Co.) for Windows (Microsoft).

RESULTS

Patient Characteristics and ^{18}F-GP1 PET/CT Procedures

Twenty-one patients were enrolled at Asan Medical Center between August 2016 and September 2017. One patient was excluded from the full analysis set because of a major protocol deviation related to an inadequate PET/CT data acquisition. Ten patients with acute DVT and 10 patients with acute PE were included for full analysis. Thromboembolic foci were confirmed by ultrasonography (n = 1) or CT venography (n = 10) for acute DVT and by CT pulmonary angiography (n = 10) for acute PE. Blood samples could not be obtained for pharmacokinetic analyses from one DVT patient after ^{18}F-GP1 injection.

The patient characteristics are listed in Table 1. All patients were on heparin, enoxaparin, warfarin, or factor Xa inhibitor treatment since their diagnosis at the time of ^{18}F-GP1 PET/CT imaging. Eight of the 10 patients presenting with acute DVT underwent CT pulmonary angiography, which revealed additional PEs in 5 of these patients. Eight of the 10 patients with acute PE were also examined for DVT by ultrasonography (n = 1) or CT venography (n = 7), which identified additional DVTs in 7 of these patients. Standard imaging studies found DVT in 76 veins of 17 patients and PE in 245 pulmonary artery territories of 15 patients.

The average interval between standard diagnostic imaging studies for DVT or PE and ^{18}F-GP1 PET/CT was 3.0 ± 1.1 d. The mean administered activity was 247.3 ± 4.4 MBq (range, 240.5–255.3 MBq), and the mean administered mass dose was 1.8 ± 2.3 μg (range, 0.2–4.4 μg).

Safety

^{18}F-GP1 administration and PET/CT procedures were well tolerated in all patients. No clinically relevant change in safety parameters was observed. There were no adverse events related to the study drug.

TABLE 1
Baseline Characteristics of Patients with Acute DVT or PE

Characteristic	DVT ($n = 10$)	PE ($n = 10$)	Total
Demographic			
Age (y)	59.9 ± 13.8	58.4 ± 18.1	59.2 ± 15.7
Male sex	5 (50%)	4 (40%)	9 (45%)
Non-Hispanic/Latino and Asian (Korean)	10 (100%)	10 (100%)	20 (100%)
Clinical feature			
Duration of signs and symptoms (d)*	18.8 ± 11.4	9.5 ± 8.7	14.2 ± 11.0
Active cancer	1 (10%)	1 (10%)	2 (10%)
Paralysis, paresis, or recent immobilization	1 (10%)	None	1 (5%)
Recently bedridden > 3 d or major surgery	3 (30%)	1 (10%)	4 (20%)
Estrogen use by women	None	1 (10%)	1 (5%)
Body mass index ≥ 30 kg/m^2	1 (10%)	2 (20%)	3 (15%)
Laboratory test (D-dimer [µg/mL FEU])	9.7 ± 5.4	7.0 ± 4.7	8.4 ± 5.1
Treatment before ^{18}F-GP1 PET/CT			
Duration of anticoagulant therapy (d)†	2.8 ± 1.1	3.2 ± 1.1	3.0 ± 1.1
Prior antiplatelet therapy	4 (40%)	1 (10%)	5 (25%)

*Duration before ^{18}F-GP1 PET/CT.
†Duration of anticoagulation therapy before ^{18}F-GP1 PET/CT or interval between standard imaging studies and ^{18}F-GP1 PET/CT.
FEU = fibrinogen-equivalent units.
Qualitative data are expressed as numbers, followed by percentages in parentheses; continuous data are expressed as mean ± SD.

Biodistribution and Pharmacokinetics of ^{18}F-GP1

^{18}F-GP1 PET/CT images showed high initial uptake in the spleen, kidneys, and blood pool, followed by a rapid clearance until 120 min ($P < 0.001$, Figs. 1 and 2A). At 120 min after injection, SUV$_{mean}$ was less than 1.5 for major organs. ^{18}F-GP1 activity was cleared by hepatobiliary and urinary excretion, with increasing activity over 120 min in the gallbladder, intestine, and urinary bladder (Fig. 2A). No focal or elevated uptake was observed in the brain, muscle, or surfaces of cortical or trabecular bones. The SUV$_{mean}$ of thromboemboli peaked early, but the time-dependent distribution of ^{18}F-GP1 differed significantly between DVT and PE (Fig. 1, $P < 0.001$). The SUV$_{mean}$ of DVT remained constant, without significant change ($P = 0.08$), but that of PE decreased until 7 min after injection ($P = 0.002$), afterward remaining stable and without further changes. The SUV$_{mean}$ ratio of thromboemboli to blood pool increased significantly until 120 min: 3.2 ± 0.7 at 60 min and 4.9 ± 1.4 at 120 min in DVT ($P < 0.001$); 2.2 ± 0.8 at 60 min and 3.7 ± 1.5 at 120 min in PE ($P < 0.001$). The plasma pharmacokinetic parameters are summarized in Supplemental Table 4. Radiolabeled metabolites were not detected in the plasma.

^{18}F-GP1 Uptake in DVT and PE

Overall image quality was adequate for interpretation in all patients from the full analysis set. ^{18}F-GP1 uptake in thromboemboli was easily distinguishable from blood-pool activity from 60 min after injection (Figs. 2 and 3, Supplemental Figs. 2 and 3). ^{18}F-GP1 PET/CT images acquired at 120 min after injection were used for analysis of the detection rate. ^{18}F-GP1 PET/CT identified thromboembolic foci in all patients enrolled with acute DVT and acute PE. When we included the 7 patients with DVT and 5 with PE who had been additionally identified by further

imaging studies, ^{18}F-GP1 PET/CT was found to detect DVT in 16 of 17 patients and PE in 15 of 15 patients (Supplemental Table 5). The false-negative ^{18}F-GP1 scan was from a patient with dyspnea and chest discomfort 1 wk after a total-knee arthroplasty. CT venography revealed 1 segmental thrombosis in the left calf
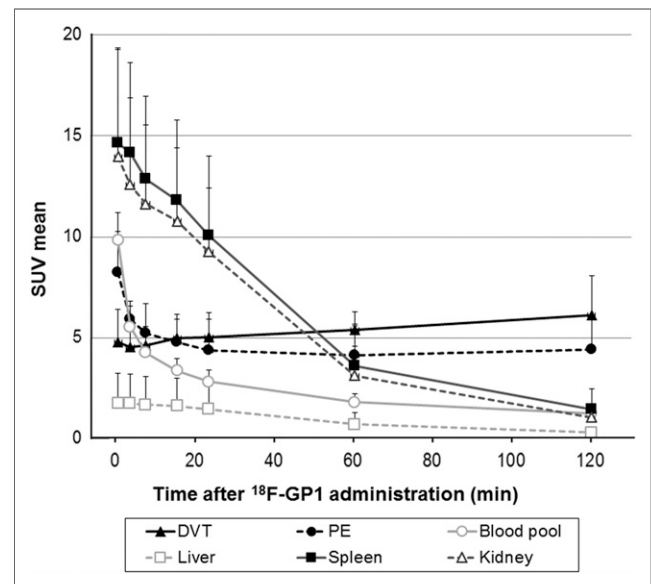
FIGURE 1. ^{18}F-GP1 biodistribution as function of time. Kidney, spleen, and blood-pool activities show high initial uptake followed by gradual washout, whereas DVT and PE demonstrate rapid initial accumulation followed by plateau phase, with minimal decrease of activity until 120 min after ^{18}F-GP1 injection.
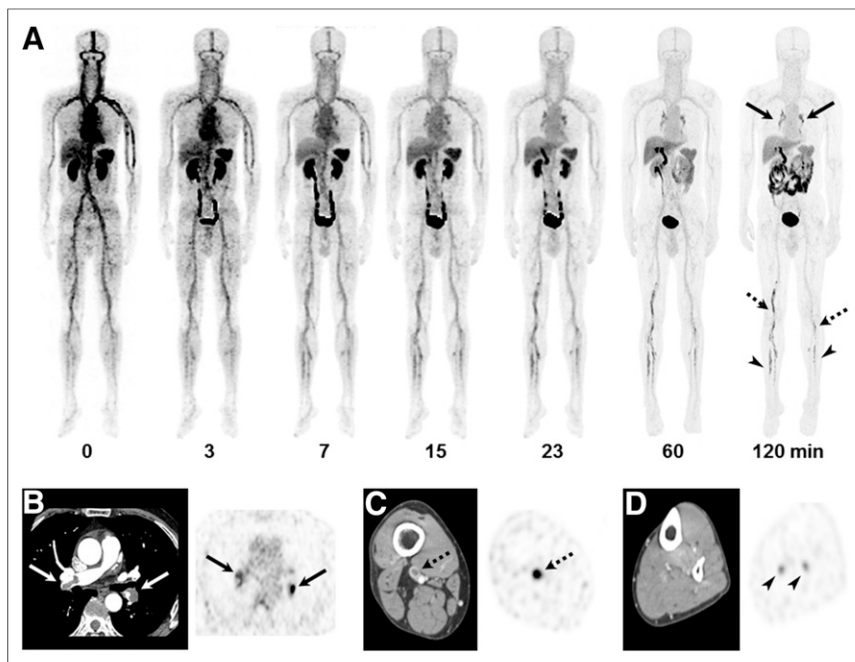
FIGURE 2. ^{18}F-GP1 PET/CT and CT images of 55-y-old man with DVT and PE. (A) Anterior maximum-intensity projections of ^{18}F-GP1 PET/CT over 120 min show positive ^{18}F-GP1 accumulation in pulmonary arteries (arrows) and in proximal (dotted arrows) and distal (arrowheads) veins of leg, which are gradually distinct on late images as ^{18}F-GP1 activity from other organs is excreted via both urinary and hepatobiliary tracts. (B–D) Transaxial CT images (left) clearly show pulmonary emboli in right main and left lower lobar pulmonary arteries (B, arrows) and thrombus in right popliteal vein (C, dotted arrow). Positive ^{18}F-GP1 uptake (right) at 120 min after injection is seen at corresponding vessels (B and C, solid and dotted arrows, respectively). Additional positive ^{18}F-GP1 uptake (right) is observed in left peroneal and gastrocnemius veins (D, arrowheads), but no corresponding filling defects are seen on CT venography (D, left).

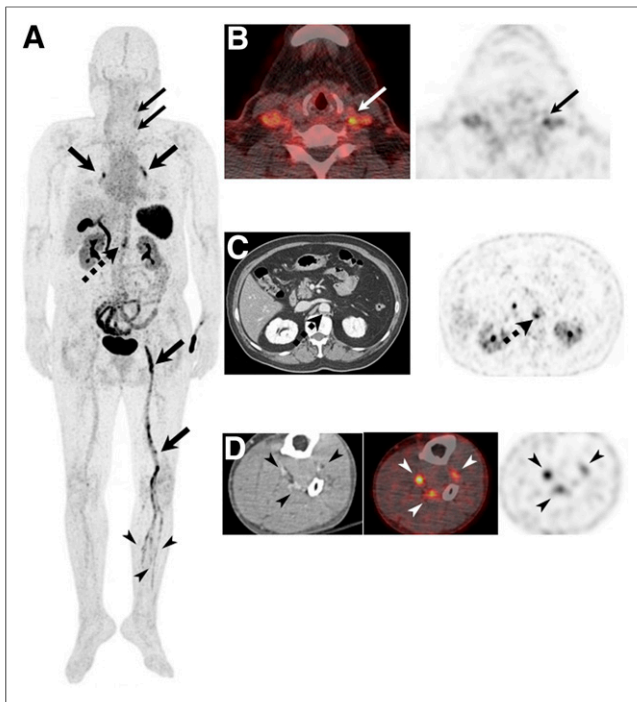### Relationship Between ^{18}F-GP1 Uptake and Clinical Characteristics

Plasma fibrinogen was elevated in 19 patients (3.8 ± 1.8 mg/mL; range, 1.6–8.4 mg/mL). P-selectin–positive platelets and procaspase-activating compound 1–positive platelets were 3.2% ± 2.8% (range, 0.3%–11.2%) and 0.2% ± 0.2% (range, 0.0%–0.6%), respectively (Supplemental Figs. 1A–1D). A positive correlation was found between the highest SUV$_{max}$ among all reference lesions at 120 min and the percentage of P-selectin–positive circulating platelets (r = 0.656, P = 0.002, Fig. 4). However, no significant correlation with other clinical or laboratory characteristics, including the duration of signs and symptoms, D-dimer level, and prior anticoagulant therapy, was observed.

DISCUSSION

The clinical results with ^{18}F-GP1 reaffirm the preclinical data from a thrombus model, as well as the favorable pharmacokinetic and safety profiles. The favorable imaging characteristics of ^{18}F-GP1 may be due to the high specificity and affinity of its parent compound, elarofiban, to its target (8), unlike arginine-glycine-aspartic acid–containing compounds, including ^{99m}Tc-apcitide (9). We postulate that nonspecific uptake of ^{18}F-GP1 in activated endothelial, smooth-muscle, and inflammatory cells is very low.

^{18}F-GP1 PET/CT showed a high detection rate for the diagnosis of VTE. However, ^{18}F-GP1 PET/CT did not diagnose one DVT patient who presented with acute PE symptoms, and not all vessels affected with VTE were ^{18}F-GP1–positive in some subjects. Platelet activation and consequent inside-out activation of GPIIb/IIIa are limited by strong inhibitory signals that prevent platelets from undesired activation and aggregation (10). If not susceptible to continued propagation, the thrombus may lyse, be detached from the vessel wall, or eventually become organized (11). Early changes may begin by 8 d after thrombogenesis (11), and the activated GPIIb/IIIa may no longer be a marker of thrombosis. All patients in this study had signs or symptoms of acute VTE within 14 d before ^{18}F-GP1 PET/CT. It is uncertain how long the process was ongoing before symptom development; patients might have had acute thromboemboli with early postthrombosis changes or old undiagnosed thromboemboli. Nonetheless, our results suggest that acute thromboemboli can be detected with ^{18}F-GP1 PET/CT up to 2 wk after symptom onset regardless of prior anticoagulation treatment. False-negative ^{18}F-GP1 PET/CT images may, in fact, indicate old VTE.

The vessel-based detection rate of ^{18}F-GP1 PET/CT was significantly lower in PE than in DVT. ^{18}F-GP1 uptake was also significantly lower in PE, which is considered to originate from embolization of DVT. Natural history studies of VTE suggest that approximately half the patients with untreated proximal DVT will develop symptomatic PE within 3 mo (12). The age of PE, therefore, might have been older than 2 mo in some of our patients, as

muscular vein, but ^{18}F-GP1 did not show uptake in the affected leg. For the vessel-based detection rate, ^{18}F-GP1 PET/CT detected 89% of the vessels with DVT and 60% with PE. The difference in the detection rate was statistically significant (P < 0.001, Supplemental Table 5). There was no difference in the vessel-level detection rate according to the location of DVT, but for PE the detection rate was significantly different (P = 0.01) in that it was lower in the segmental pulmonary artery than in the main or lobar pulmonary artery (Supplemental Table 5). Additionally, ^{18}F-GP1 PET/CT showed increased uptake in 29 veins of the lower extremity and 3 pulmonary arteries (Supplemental Table 5; Figs. 2D and 3D; Supplemental Fig. 2A), which were not detected on standard imaging. Of the 32 DVTs and PEs newly detected with ^{18}F-GP1 PET/CT, 25 were in distal veins of the lower extremity in 12 patients, which included 9 newly detected DVTs in 4 patients (3 presented with acute DVT and 1 with acute PE) that had no distal DVTs on standard imaging. Interestingly, ^{18}F-GP1 PET/CT demonstrated increased uptake in locations with recent trauma (Supplemental Figs. 2A, 2C, and 2D), in the common carotid artery (Fig. 3A and 3B), in the abdominal aorta (Fig. 3C), and in the right atrium (Supplemental Figs. 4A–4C).

For lesion-based quantitative analysis, 43 lesions with DVT and 50 with PE were defined as reference lesions. The SUV$_{max}$ of the reference lesions at 60 and 120 min after injection was 5.1 ± 2.4 and 5.2 ± 2.9, respectively, for DVT (P = 0.49) and 4.1 ± 2.0 and 4.1 ± 2.1, respectively, for PE (P = 0.56), with a statistical difference observed between DVT and PE (P < 0.05).

FIGURE 3. ^{18}F-GP1 PET/CT and CT images of 69-y-old woman with DVT and PE. (A) Anterior maximum-intensity projection of ^{18}F-GP1 PET/CT at 120 min after injection shows multiple areas of increased uptake in both pulmonary arteries and veins of left lower extremity at DVT and PE sites (thick arrows), as well as foci of abnormal ^{18}F-GP1 uptake in left common carotid artery (thin arrows); left anterior tibial, posterior tibial and peroneal veins (arrowheads); and abdominal aorta (dotted arrow). (B–D) Foci of abnormal ^{18}F-GP1 uptake are seen in left common carotid artery (B, right, arrow); abdominal aorta (C, right, dotted arrow); and left anterior tibial, posterior tibial, and peroneal veins (D, middle and right, arrowheads). Contrast-enhanced CT images reveal low-density, noncalcified plaque in abdominal aorta (C, left, dotted arrow) but no filling defects in distal veins of left lower extremity (D, left, arrowheads). No further imaging studies were performed to characterize left carotid uptake.

demonstrated in a previous histologic study (*13*). Additionally, the shedding of large emboli may be associated with inhibition of platelet and coagulation activation necessary for thrombus stability (*14*). These mechanisms may explain the observed difference between DVT and PE. The effect of the age of a thrombus and the heterogeneity of its formation and stabilization on ^{18}F-GP1 uptake and the diagnostic performance need to be further explored.

Interestingly, ^{18}F-GP1 PET/CT showed additional increased uptake in distal veins of the lower extremities in this study. Improved detection of distal DVT might be important, because about 25% of untreated symptomatic calf DVTs extend to the proximal veins, mostly within 1 wk of presentation, and may cause PE (*12,15*). The positive uptake without corresponding abnormal findings on standard imaging modalities may indicate a more sensitive detection of DVT in the distal veins. Venous ultrasound is the first-line DVT imaging modality, but CT venography was performed as a standard imaging test in most patients in this study. CT venography has not been well validated for the diagnosis of distal DVT (*5,16*). Furthermore, because of the nature of this phase 1 study, no subjects without diagnosed DVT or PE were enrolled, and the specificity of ^{18}F-GP1 PET/CT therefore could not be evaluated.

We cannot conclude that ^{18}F-GP1 PET/CT is more sensitive in detecting acute DVT in the distal veins. It is difficult to assess whether the distal lesions represent clinically significant occlusive DVT or simply activated platelets adhering to the vessel wall. The data obtained with ^{18}F-GP1 so far are consistent with the fact that many of the DVTs start in the distal vessels and propagate proximally. The diagnostic accuracy for distal DVT and the utility in identifying individuals who would benefit from anticoagulation for distal DVT need to be assessed in future studies.

Although the current study was not designed to assess thrombi other than VTE, the nature of a whole-body scan allowed us to document additional thrombotic events, albeit anecdotally. For example, 1 patient presented after a syncopal episode resulting in knee and chin lacerations and a mandible fracture—all 3 of these traumatic blood clots, in addition to the DVT and bilateral PEs, were visualized by ^{18}F-GP1 PET/CT. In other subjects, the lesions that were visualized might have been consistent with a right atrial thrombus or with atherosclerotic lesions in the carotid arteries and abdominal aorta. These findings suggest possible future applications for ^{18}F-GP1 in imaging of atherosclerotic plaque rupture and thrombosis.

We found that ^{18}F-GP1 uptake correlated positively with P-selectin–positive platelets but not with other clinical or laboratory markers. All enrolled patients had highly elevated D-dimer levels, and as expected, no correlation could be found between ^{18}F-GP1 uptake and D-dimer levels. The exposure of surface P-selectin is temporary because of the rapid shedding of P-selectin to the plasma and the sequestration of these activated platelets into heterotypic aggregates (*17,18*). Platelet surface P-selectin is an ideal marker for the detection of activated circulating platelets in the context of ongoing thrombosis (*19*). The percentage of activated platelets with P-selectin expression as assessed by flow cytometry is regarded as the gold standard for acute or continuous platelet activation (*19,20*). Thus, our results suggest that ^{18}F-GP1 uptake is associated with acute, but
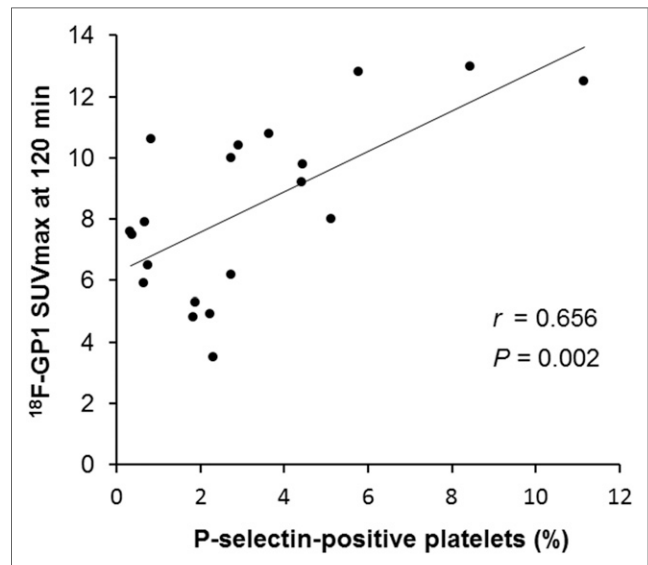
FIGURE 4. Relationship between P-selectin expression on circulating platelets and ^{18}F-GP1 uptake. Scattergram shows positive correlation between highest SUV$_{max}$ of ^{18}F-GP1 among all reference lesions at 120 min after injection and percentage of P-selectin–positive platelets measured by flow cytometry using CD62P monoclonal antibody.

not chronic, VTE. On the other hand, another marker of activated platelets, procaspase-activating compound 1, was very low in all patients. Procaspase-activating compound 1 flow cytometry may not identify the subtle changes in platelet activation status (*21*). Lastly, whereas elevated fibrinogen could competitively inhibit ^{18}F-GP1 binding to activated platelets, we observed that ^{18}F-GP1 uptake in thromboemboli was not significantly affected by the fibrinogen level.

This study has several limitations. The high detection rate should be interpreted with caution regarding the small number of patients and the inclusion criteria, which allowed only patients with overt symptoms and signs of acute VTE to be included. In addition, no imaging or clinical follow-up data were available to discriminate between true- and false-positive ^{18}F-GP1 uptake in the distal veins. In the absence of a control group of patients with symptoms consistent with DVT/PE without imaging evidence of DVT/PE, the specificity of ^{18}F-GP1 uptake remains uncertain. Finally, thrombus formation is a dynamic process, and the properties of thrombi differ according to time and region (*22*). Therefore, the ^{18}F-GP1 uptake measured at a single time point would represent only a snapshot in the disease process and cannot represent the thrombus heterogeneity.

CONCLUSION

^{18}F-GP1 is a safe and promising novel PET tracer for imaging acute VTE, with favorable biodistribution and pharmacokinetics in patients. By using ^{18}F-GP1, which targets an intrinsic pathologic molecular event in thrombus formation, it is possible to detect acute thromboemboli within the whole body without contrast medium. ^{18}F-GP1 PET/CT may identify thrombi in distal veins of the leg, where conventional imaging has limitations. A positive correlation between ^{18}F-GP1 uptake and P-selectin–positive platelets suggests that ^{18}F-GP1 PET/CT may be helpful in differentiating acute VTE from chronic VTE. Taken together, the findings of this study indicate that ^{18}F-GP1 PET/CT may provide an opportunity to overcome the limitations of current diagnostic strategies for acute VTE.

DISCLOSURE

REFERENCES

1. Heit JA. Epidemiology of venous thromboembolism. *Nat Rev Cardiol.* 2015;12: 464–474.
2. Elliott CG, Goldhaber SZ, Jensen RL. Delays in diagnosis of deep vein thrombosis and pulmonary embolism. *Chest.* 2005;128:3372–3376.
3. Cohen AT, Agnelli G, Anderson FA, et al. Venous thromboembolism (VTE) in Europe: the number of VTE events and associated morbidity and mortality. *Thromb Haemost.* 2007;98:756–764.
4. Bates SM, Jaeschke R, Stevens SM, et al. Diagnosis of DVT: antithrombotic therapy and prevention of thrombosis, 9th ed: American College of Chest Physicians evidence-based clinical practice guidelines. *Chest.* 2012;141:e351S–e418S.
5. Thomas SM, Goodacre SW, Sampson FC, van Beek EJ. Diagnostic value of CT for deep vein thrombosis: results of a systematic review and meta-analysis. *Clin Radiol.* 2008;63:299–304.
6. Cogo A, Lensing AW, Prandoni P, Hirsh J. Distribution of thrombosis in patients with symptomatic deep vein thrombosis: implications for simplifying the diagnostic process with compression ultrasound. *Arch Intern Med.* 1993;153:2777–2780.
7. Kyrle PA. How I treat recurrent deep-vein thrombosis. *Blood.* 2016;127:696–702.
8. Lohrke J, Siebeneicher H, Berger M, et al. ^{18}F-GP1, a novel PET tracer designed for high-sensitivity, low-background detection of thrombi. *J Nucl Med.* 2017;58:1094–1099.
9. De Corte BL, Kinney WA, Liu L, et al. Piperidine-containing beta-arylpropionic acids as potent antagonists of alphavbeta3/alphavbeta5 integrins. *Bioorg Med Chem Lett.* 2004;14:5227–5232.
10. Broos K, Feys HB, De Meyer SF, Vanhoorelbeke K, Deckmyn H. Platelets at work in primary hemostasis. *Blood Rev.* 2011;25:155–167.
11. Wakefield TW, Myers DD, Henke PK. Mechanisms of venous thrombosis and resolution. *Arterioscler Thromb Vasc Biol.* 2008;28:387–391.
12. Kearon C. Natural history of venous thromboembolism. *Circulation.* 2003;107: I22–I30.
13. Fineschi V, Turillazzi E, Neri M, Pomara C, Riezzo I. Histological age determination of venous thrombosis: a neglected forensic task in fatal pulmonary thrombo-embolism. *Forensic Sci Int.* 2009;186:22–28.
14. Cosemans JM, Angelillo-Scherrer A, Mattheij NJ, Heemskerk JW. The effects of arterial flow on platelet activation, thrombus growth, and stabilization. *Cardiovasc Res.* 2013;99:342–352.
15. Kearon C, Akl EA, Ornelas J, et al. Antithrombotic therapy for VTE disease: CHEST guideline and expert panel report. *Chest.* 2016;149:315–352.
16. Mazzolai L, Aboyans V, Ageno W, et al. Diagnosis and management of acute deep vein thrombosis: a joint consensus document from the European Society of Cardiology working groups of aorta and peripheral circulation and pulmonary circulation and right ventricular function. *Eur Heart J.* February 17, 2017 [Epub ahead of print].
17. Michelson AD, Barnard MR, Hechtman HB, et al. In vivo tracking of platelets: circulating degranulated platelets rapidly lose surface P-selectin but continue to circulate and function. *Proc Natl Acad Sci USA.* 1996;93:11877–11882.
18. Michelson AD, Barnard MR, Krueger LA, Valeri CR, Furman MI. Circulating monocyte-platelet aggregates are a more sensitive marker of in vivo platelet activation than platelet surface P-selectin: studies in baboons, human coronary intervention, and human acute myocardial infarction. *Circulation.* 2001;104:1533–1537.
19. Michelson AD, Furman MI. Laboratory markers of platelet activation and their clinical significance. *Curr Opin Hematol.* 1999;6:342–348.
20. Kappelmayer J, Nagy B Jr, Miszti-Blasius K, Hevessy Z, Setiadi H. The emerging value of P-selectin as a disease marker. *Clin Chem Lab Med.* 2004;42:475–486.
21. McCabe DJ, Harrison P, Mackie IJ, et al. Platelet degranulation and monocyte-platelet complex formation are increased in the acute and convalescent phases after ischaemic stroke or transient ischaemic attack. *Br J Haematol.* 2004;125:777–787.
22. Munnix IC, Cosemans JM, Auger JM, Heemskerk JW. Platelet response heterogeneity in thrombus formation. *Thromb Haemost.* 2009;102:1149–1156.